ARTICLE IN PRESS



Available online at www.sciencedirect.com



Journal of Marine Systems xx (2004) xxx-xxx



www.elsevier.com/locate/jmarsys

Particle tracking method in the approach for prediction of oil slick transport in the sea: modelling oil pollution resulting from river input

K.A. Korotenko^{a,b,*}, R.M. Mamedov^c, A.E. Kontar^b, L.A. Korotenko^b

^a Thayer School of Engineering, Dartmouth College, 8000 Cummings Hall, Hanover, NH 03755-8000, USA
 ^b P.P. Shirshov Institute of Oceanology, 36 Nakhimovskiy pr., Moscow 117851, Russia
 ^c Institute Geography of Azerbaijan Academy of Sciences, 31 Javida, Baku 370143, Azerbaijan

Received 2 September 2002; received in revised form 10 July 2003; accepted 5 November 2003

Abstract

A 3-D hybrid flow/transport model has been developed to predict the dispersal of oil pollution resulting from river discharges. The transport module of the model takes predetermined current and turbulent diffusivities and uses Lagrangian tracking to predict the motion of individual particles (droplets), the sum of which constitutes hypothetical oil spills. Currents and turbulent diffusivities used in the model have been generated by a numerical ocean circulation model (POM) implemented for the Caspian Sea. The basic processes affecting the fate of the oil spill are taken into account and parameterised in the transport model. The process of evaporation is modelled with a new technique based on the pseudo-component approach.

The model is used to simulate a continuous oil release from the Volga river into the coastal waters of the north part of the Caspian Sea. Oil slick movement and risk of contamination of the coastline by beaching oil spills are illustrated for different wind conditions.

© 2004 Published by Elsevier B.V.

Keywords: Caspian Sea; Oil spill; River discharge; Particle tracking technique

1. Introduction

The Caspian is the largest inland body of water on the planet, with a surface area of 384,400 km², volume of 78,700 km³, and a coastline nearly 7000 km long. It measures 1200 km from north to south and 200–450 km from east to west. The Sea (Fig. 1)

extends zonally from 46.6° to 54.8°E and meridionally from 36.6° to 47.0°N. Over 60% of the Sea is shallower than 100 m. There are two relatively deep basins (about 600 and 900 m, respectively) in the central and southern parts of the sea. The shelf zone is very wide, and steep slopes occur only in the two deep basins. The Caspian Sea is an enclosed sea with major freshwater input from the Volga River balanced by evaporation. The dynamics of the Caspian Sea is dominated by mesoscale signals triggered by baroclinic processes and interactions with the very irregular bathymetry. There is however a wide variety of processes in the sea, e.g., interactions between shelf

0924-7963/\$ - see front matter © 2004 Published by Elsevier B.V. doi:10.1016/j.jmarsys.2003.11.023

^{*} Corresponding author. P.P. Shirshov Institute of Oceanology, 36 Nakhimovskiy pr., Moscow 117851, Russia. Tel.: +7-95-218-21147; fax: +7-95-124-5983.

 $[\]hbox{\it E-mail address:} \ Konstantin. Korotenko@Dartmouth. Edu (K.A. Korotenko).$

K.A. Korotenko et al. / Journal of Marine Systems xx (2004) xxx-xxx

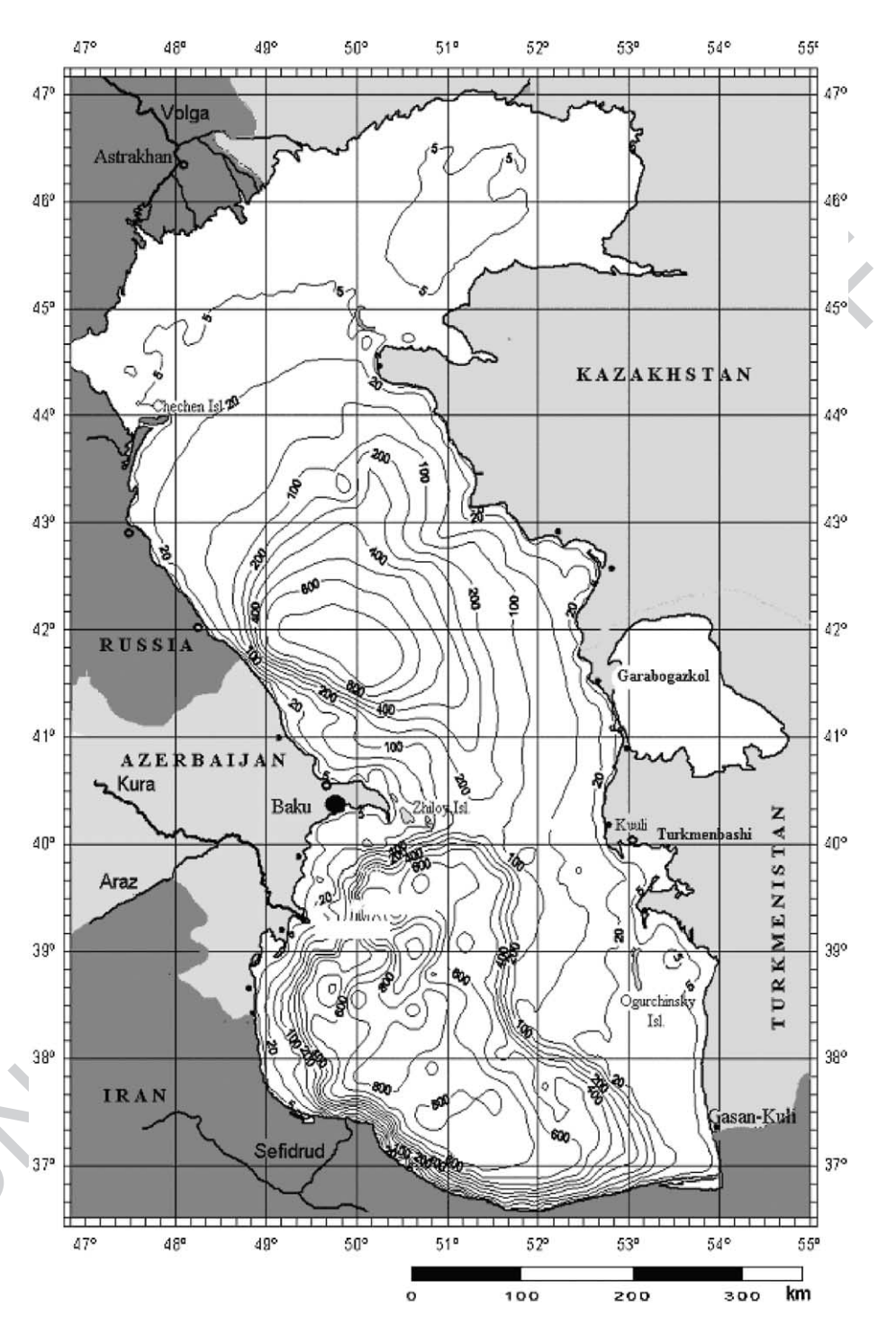


Fig. 1. The Caspian Sea bathymetry.

K.A. Korotenko et al. / Journal of Marine Systems xx (2004) xxx-xxx

Sources	Oil, tons/
	year
Rivers	75,000
Municipalities	19,000
Industries	28,000
Atmosphere	350
Total	122,350

t1 1

Table 1

and deep basin circulation, deep basin ventilation, and ice dynamics.

In the Caspian Sea, salinity varies from zero in the shallow northern part (in vicinity of the Volga river discharge zone) to 14 ppt in the southeastern part. In general, salinity increases with longitude and depth. Mean temperature has large meridional and seasonal variations of up to 27 °C in summer to zero in winter. A relatively shallow seasonal thermocline occurs at depths of 10–40 m, and is absent in winter. Salinity and temperature in the bottom layer of the two deep basins are almost constant and average about 13 ppt,

4 °C and 12 ppt, 6 °C, respectively, for the central and southern basins. Detailed analysis of physical properties and dynamics of the Caspian Sea are given in Korotenko et al. (2002).

The Caspian Sea is fed by numerous rivers, but the Volga River alone contributes about 82% of the annual input.

The Caspian is considered to have three sections: north, middle, and south. The extreme northern end is relatively shallow (~ 5 m average depth) when compared to the southern part (900 m average depth). Oil production, industry, and transportation have caused severe air, water, and soil pollution problems in the Caspian region. The Volga is a major (but not the only) conduits of pollutants to the Caspian Sea including oil pollution. The estimated amount of the input is given in Table 1. According to these data the total amount of oil discharged by Caspian rivers reaches about 75,000 tons/year and, among the rivers, the Volga input is the largest one with 95% of the total petroleum hydrocarbons input.

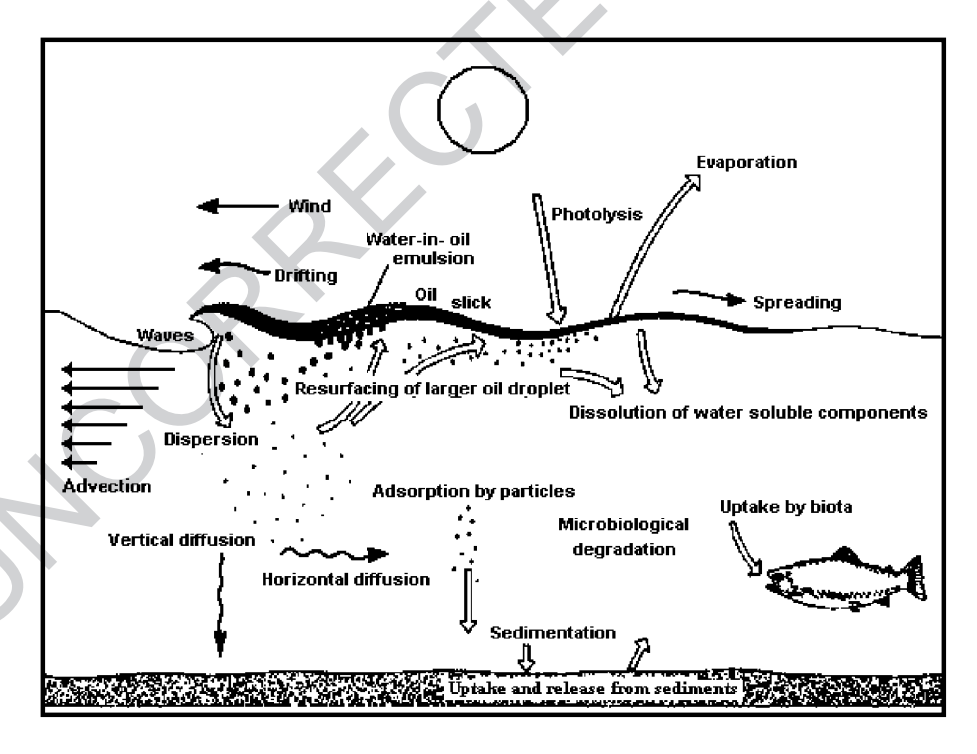


Fig. 2. Processes affecting the oil slick (modified from Daling et al., 1990).

Once oil is discharged at the sea surface, it is transported by the flow and affected by many processes such as evaporation, emulsification, dissolution, photolysis, biodegradation, etc., that depend on the properties of the oil. Fig. 2 shows the most important such mechanisms affecting an oil slick in the marine environment. The accurate simulation of the fate of oil slicks also requires a good knowledge of the environmental conditions, e.g., winds, currents, waves, turbulence, salinity, temperature, and solar insolation. Surface winds and currents are the most important factors determining the direction and rate at which an oil slick moves. The physical, chemical, and biological reactions, which weather or modify oil as it drifts and spreads, take place over various time scales ranging from a few hours to months and even years. The main aspects of this dynamics have been summarised by Mackay and McAuliffe (1988), Spaulding (1988), and Korotenko et al. (2001, 2002, 2003).

Practical implementations of different approaches to oil spill modelling can be found in a large number of papers (e.g. Lehr et al., 1981; Belen et al., 1981; Proctor et al., 1994; Varlamov et al., 1998; Cekirge and Palmer, 2001; Korotenko et al., 2001, 2002, 2003).

This paper is structured as follows: In Section 2, the structure of the model proposed for modelling oil

spills and its implementation for the Caspian Sea are described. Results of simulations of oil slick resulting from the Volga river discharge for different wind conditions are analysed in Section 3. A short summary is given in Section 4.

2. Oil spill model

The presented model uses the random walk (also called Monte Carlo) technique to follow the motion of individual particles (oil droplets), the total amount of which constitutes the oil spill. Models based on the random walk concept are significantly more effective (Hunter, 1987) than the finite-difference models mainly because they describe exactly the advection, which is a very important transport process for oil slicks. The model consists of two main modules: transport and hydrodynamic. The modules are described below.

2.1. Transport model

The basic concept of this approach (Fig. 3) is similar to that of Proctor et al. (1994), except that oil is initially divided into fractions in order to describe the evaporation process with more accuracy.

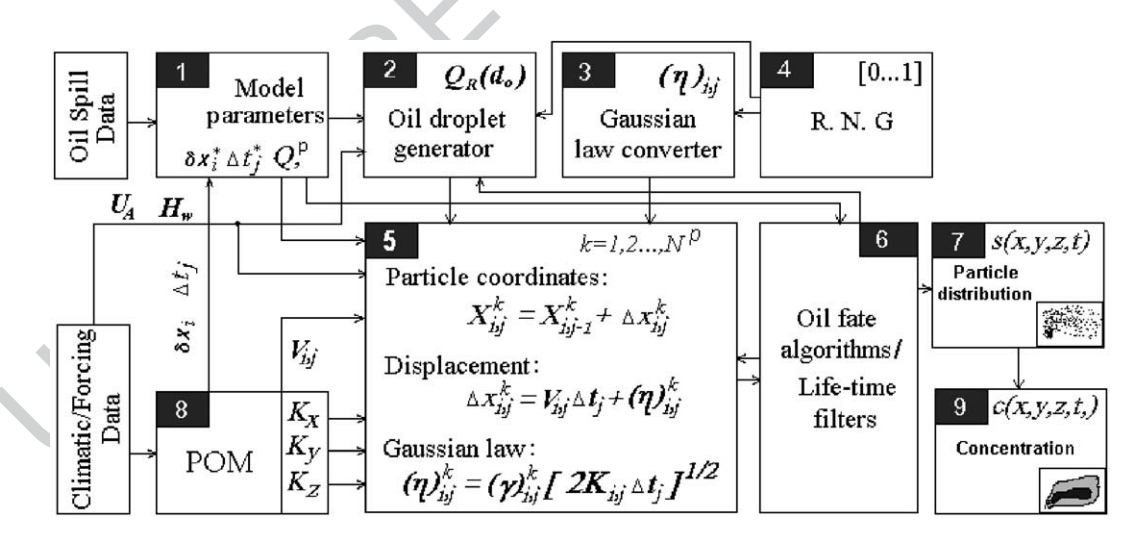


Fig. 3. Range of contents for hydrocarbon fractions (left) and the percent weight changes of individual fraction of a light crude oil versus time (right) (modified from Yang and Wang, 1977).

145

146

147

148

149

150

151

152

153

154

155

156

157

158

159

160

161

K.A. Korotenko et al. / Journal of Marine Systems xx (2004) xxx-xxx

130 The main part of the model is Block 5 where 131 displacements of each particle are estimated by 132 (Korotenko, 1994):

$$(\Delta x_i)_{j,k} = V_{i,j} \ \Delta t_j + (\eta_i)_{j,k}$$

$$(i = 1 - 3; \ j = 1, 2, \dots, N_t; \ k_f = 1, 2, \dots, N_f;$$

$$f = 1, 2, \dots, 8)$$
(1)

134

135

136

137

138

139

142

The displacements $(\Delta x_i)_{j,k}$ are defined as the deterministic part of the motion due to the mean velocity field, $V_{i,j}$ and the random displacement, $(\eta_i)_{j,k}$ due to fluctuations of the velocity and denotes the displacement of the kth particle moving along the xi axis at the jth instant of time, Nt is the number of time steps, Δt is the time step, N_f is the number of particles in each fraction, and the subscript f denotes a particle fraction.

The distribution of the number of particles in fractions (hydrocarbon groups) is initially assigned and distributed randomly depending on the type of oil. The total number of the particles launched in the model usually does not exceed 106; nevertheless, the behavior of the tracked particles proved to be representative of the entire spill, even though each droplet represents only a small part of the total volume of the oil. Within each fraction, each droplet is also randomly distributed to have its own half-life according to the empirical exponential laws (Fig. 4, right). In practice, those distributions are assigned randomly by means of a random number generator giving uniform numbers chosen uniformly between 0 and 1, and then they are transformed into an exponential distribution with a weight dependent on wind speed and oil temperature. The 'long-living' fractions such as C^2 , C^4 , C^6 , C^7 , and C⁸ are randomly exponentially distributed within a

Description	Density, g/ml	Boiling Point, C	Molecular Weight
Paraffin C ₆ -C ₁₂	0.66- 0.77	69-230	86-170
Paraffin C ₁₃ -C ₂₅	0.77- 0.78	230- 405	184-352
Cycloparaffin C ₆ -C ₁₂	0.75-0.9	70-230	84-164
Cycloparaffin C ₁₃ -C ₂₃	0.9-1.0	230- 405	156-318
Aromatic (mono and di-cyclic) C ₆ -C ₁₁	0.88-1.1	80-240	78-143
Aromatic (poli -cyclic) C ₁₂ -C ₁₈	1.1-1.2	240- 400	128-234
Naphtheno- aromatic C ₉ -C ₂₅	0.97-1.2	180- 400	166-300
Residual (includuding heterocycles)	1.0-1.1	400	300-900

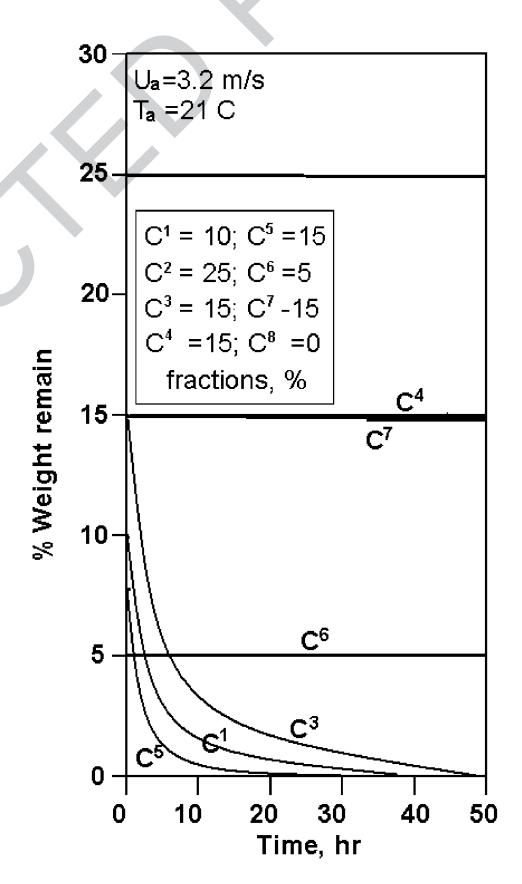


Fig. 4. Schematic of principal elements of the hybrid model.

range corresponding to the rather slow effect of total degradation. Their half-life for total degradation is chosen to be 250 h (Proctor et al., 1994).

In addition to the regular movements due to the mean current, oil droplets experience a random diffusion due to the velocity fluctuations, the distribution law of which is represented by the term, $(\eta_i)_{i,k}$, the latter being, in the general case, a function of time and space. The type of law for $(\eta_i)_{j,k}$ is determined by the statistical structure of deviations (fluctuations) of the velocity from its mean value at each time step Δt . Since these fluctuations are considered independent, the law for $(\eta_i)_{i,k}$ is thought to be Gaussian (Monin and Yaglom, 1965). In this case, the $(\eta_i)_{j,k}$ can be represented as $(\eta_i)_{i,k} = \gamma_{i,k} (2K_{i,j}\Delta t)^{1/2}$, where $\gamma_{i,k}$ is a random vector normally distributed with an averaged value of zero and unit standard deviation; $K_{i,k}$ represents the diffusion coefficient along the x_i axis at time $t_i = t_0 + j\Delta t$. The random vector, $\gamma_{i,k}$, is obtained with the use of the random number generator, Block 4, giving a homogeneous distribution of random numbers between 0 and 1, with consequent transformation to the Gaussian law in Block 3. The horizontal and vertical diffusion coefficients, $K_{x,j}$, $K_{y,j}$, and $K_{z,j}$, as well as the mean current velocity U_i^J are provided by the flow model, Block 8. In the presented version of the model, the horizontal diffusion coefficients, $K_{x,i}$ and $K_{y,j}$, were calculated in POM from Smagorinsky formula, while the vertical diffusivity, $K_{z,j}$, was obtained from the level 2.5 turbulence model (Mellor and Yamada, 1982).

In the 'Oil Spill Data' block, the location and configuration of source(s), its (their) regime of release and production rate, and type of oil and hydrocarbon groups are collected for subsequent initialization in Block 1, where initial parameters such as the size of the investigated area, spatial resolution and time steps are adjusted to those used in the flow model, Block 8.

In Block 2, the particles' diameter, d_0 , is assigned randomly in the range $d_{\rm max}-d_{\rm min}$. The entrainment rate, $Q_{\rm R}(d_0)$, is defined as a function of $U_{\rm A}$ and $H_{\rm rms}$ (Eq. (4)). The critical diameter, $d_{\rm c}$ (Aravamudan et al., 1982), is given by the expression $d_{\rm c}=9.52{\rm v}^{2/3}/(g^{2/3}(1-\rho_0/\rho)^{1/3})$. The buoyancy force depends on the density and size of the droplets and the vertical velocity, w (Proctor et al., 1994), which can be estimated as $w=(gd^2(1-\rho_0/\rho))/18v$ for small droplets $d \le d_{\rm c}$, and as $w=((8/3)gd(1-\rho_0/\rho))^{1/2}$ for large drop-

lets $d > d_c$. Hence, the larger droplet sizes are more buoyant and tend to remain near the sea surface, while the smaller droplets are less buoyant and could be transported downwards due to turbulence. Each particle, droplet or slicklet k belonging to fraction f is characterized by its size, density, position $X_{i,j}^k$, age, and its own 'half-life', the latter being assigned a priori when the particle is launched.

The transport model includes the effects of evaporation, emulsification, and decomposition, the latter due to biochemical and physical degradation. Algorithms for these effects are incorporated in Block 6, and they are parameterized in terms of 'half-life' time filters, which compare current time and the 'half-life' time assigned for each particle. Only particles that occur within the subsurface 'evaporation layer' of thickness, $z_{\rm ev}$ (0.1 m), experience evaporative decay, while particles at all depths in the water column experience disintegration.

The model takes into account the beaching of oil: If the oil droplet reaches the coastline, it is marked as beached. In this case, the droplet is fixed at the point where it reached the beach; otherwise, the droplet is reflected back to sea and remains in the computational process.

Finally, data of coordinates $S_j = \{(X_1; X_2; X_3)_j\}$ are stored in Block 7, the latter being also used for identification of space cells where each particle is found at time t_j . The particle concentration C(x,y,z,t) in a cell is defined in Block 9 as the number of particles found in the cell relative to the volume of the cell. In this block, the particles remaining in the water column, at the sea surface, beached, and decayed are counted separately and inventoried in an updated summary.

Operationally, the hybrid model is controlled primarily by "Oil Spill Model" Dialog with a map of the Caspian Sea shown in Fig. 5. The model is started with "Update and Run" button, which reads in bathymetry, predetermined current velocities, and model and source parameters. A source position is determined by the mouse pointer location; in doing so the Lat/Long coordinates and instantaneous depth will be displayed. The user may choose whether the spill is bulk or continuous, and specifies the period of spill in the later case. Once the model is running, the user may also specify the wind and wave conditions as well as choose which fraction (evaporated,

K.A. Korotenko et al. / Journal of Marine Systems xx (2004) xxx-xxx

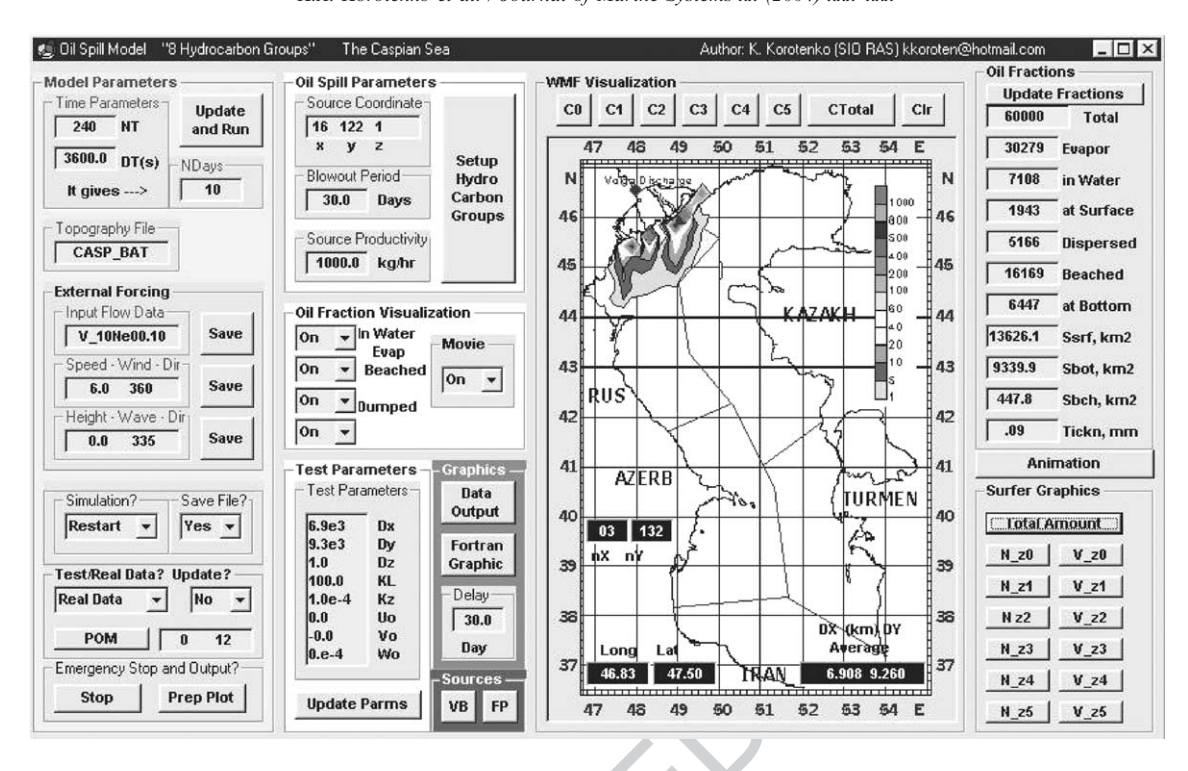


Fig. 5. Main Dialog of the oil spill model.

beached, deposited, etc.) must be displayed during the calculations. It should be noted that once "Update and Run" button is clicked, it runs a separate graphic window displays real-time motion of droplets. The concentration recalculated from particle density and oil fraction distributions during the spilling process are displayed at the map and in correspondent frames at the upper right corner of the main Dialog. A special Properties Dialog, which appears by clicking "Setup Hydrocarbon Groups" button, allows the user to input type and properties of oil.

2.2. Flow module

A high-resolution circulation model is required to describe the complex hydrodynamics and thermohydrodynamics of coastal waters and provide appropriate simulations of the detailed influence of evaporation, river discharge, and synoptic atmospheric forcing. For this purpose, the sigma-coordinate (terrain-following) primitive equation Princeton Ocean Model (POM) (Blumberg and Mellor, 1987)

has been implemented (Block 8) with horizontal and vertical resolutions of respectively, about 5 ft and 1 m (for upper layer of the sea). The model is first used to compute the climatological mean flow, V_i^c . This is done by forcing the model with monthly averaged wind stresses. In a second step, wind-driven currents, V_i^d , are computed using synoptic winds for the winter and summer seasons. In these runs, the surface stress is calculated using a wind speed dependent drag coefficient, C_A (C_A =1.1 × 10⁻³ for U_A ≤ 6.5 m/s and C_A =0.61 × 10⁻³ for U_A >6.5 m/s). The bottom stress is calculated with a drag coefficient chosen to be either dependent on grid size or constant, 0.0025, in case of a grid with low resolution (Blumberg and Mellor, 1987). Tidal currents in the Caspian Sea are negligible.

2.3. Implementation of the model for the Caspian Sea

The Princeton Ocean Model coarse grid area covers the entire Caspian Sea from 38°40′ to 47°N and from 47° to 54°E. The grid size is 1/12° in both longitudinal and latitudinal directions. It

K.A. Korotenko et al. / Journal of Marine Systems xx (2004) xxx-xxx

Wind	Wind Direction							
speed, m/s	N	NE	Е	SE	S	SW	W	NW
0	7.24	0.02	0	0	0	0	0	0
0 - 5.0	4.28	5.48	3.5	5.44	1.87	1.71	1.75	5.46
5.0 - 7.5	11.53	8.50	3.45	5.45	2.29	1.48	1.60	11.5
7.5 - 12.5	4.61	1.81	0.56	1.04	0.31	0.15	0.1	5.7
12.5 - 17.5	0.81	0.14	0	0.04	0.02	0	0	1.87
17.5 - 22.5	0.04	0	0	0	0	0	0	0.22

302 corresponds to the zonal resolution ranging from 303 6.09 km at 37°N to 7.50 km at 47°N, and a 304 meridional resolution of 9.02 km. POM has 21 305 sigma levels and was initialized with seasonally 306 averaged climatic temperature and salinity fields. 307 These seasonal characteristics were used as the

initial background condition for the calculation of short-term variations due to synoptic winds. Spinning up of the model was performed under steady southward wind 6 m/s during 3 months. The probability of occurrence of various wind directions in summer (Table 2) was used for the simulation of drift currents and oil spreading from the Volga riverdischarge. Southeastward, southward, and southwestward winds are the most prevalent winds for summer. Examples of surface drift currents generated by steady southward wind of 6 m/s are presented in Fig. 6. The circulation is strongest in the extensive shallow shelf areas, taking the form of coastal jets. This effect was also noted numerically (Korotenko and Mamedov, 2001; Korotenko et al., 2001, 2002). The jet-like structure of the surface currents appears along both the western and eastern boundaries. Under non-stationary wind forcing,

308

309

310

311

312

313

314

315

316

317

318

319

320

321

322

323

324

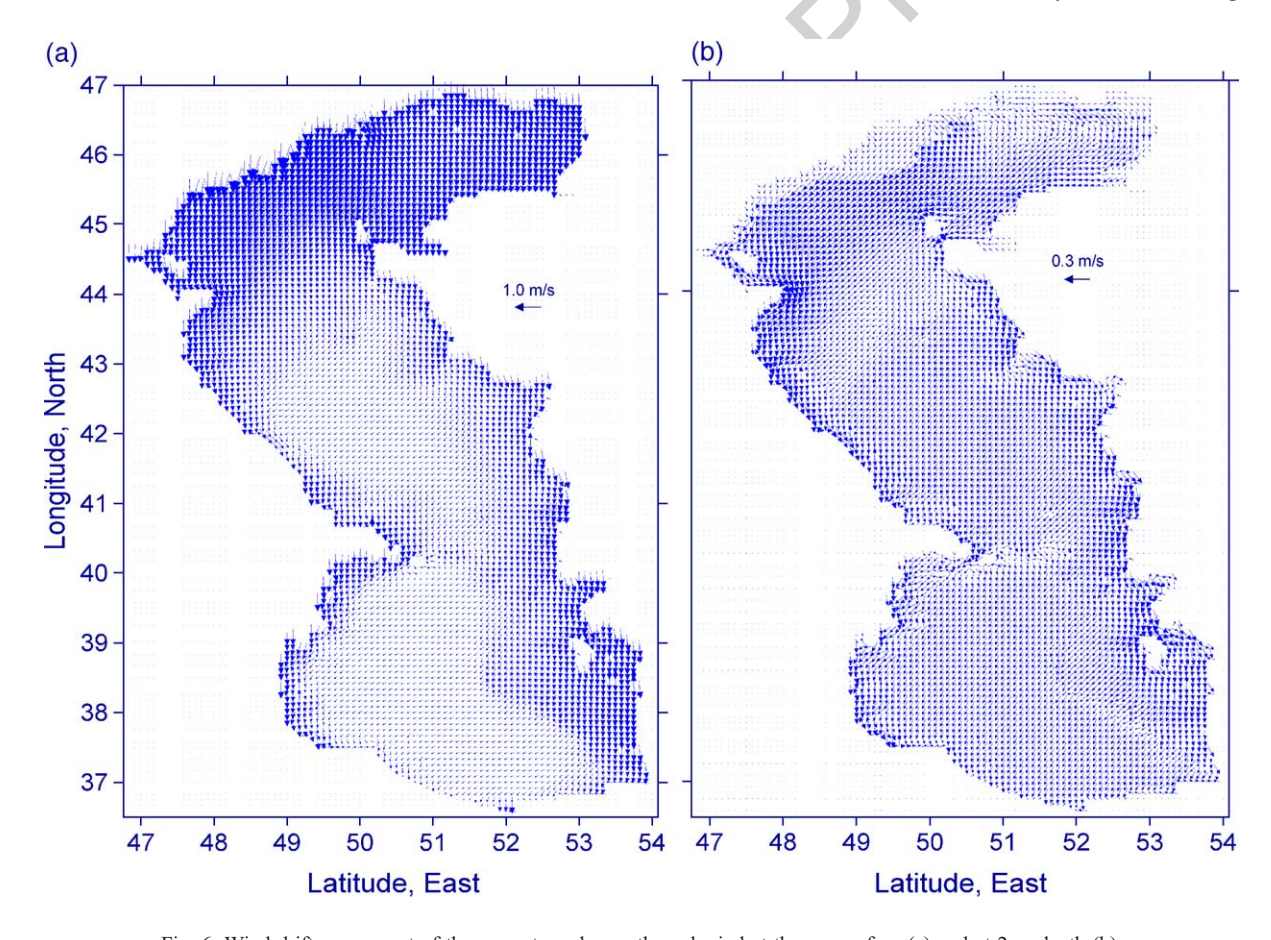


Fig. 6. Wind drift component of the currents under southward wind at the sea surface (a) and at 2 m depth (b).

strong changes in the upper layer circulation occur within a few days in numerical simulations, as has also been noted numerically by Badalov and Rzheplinsky (1989).

In the model, the Volga river fresh water input is divided into five passages to simulate fresh water plume and current velocity more realistically. The passages are treated as individual sources of freshwater which are implemented in the model's continuity equations (see Kourafalou et al., 1996). The velocity field presented in Fig. 6 shows the strong influence of this river discharge in the north part of the Caspian Sea.

3. Simulation of oil slick from the Volga river 340 **discharge**

Before simulating the transport of oil slicks, a number of initial parameters had to be specified. The oil (Gunashly type) was specified by density $\rho_{\rm oil} = 872 \, {\rm kg/m^3}$, droplet diameters, $d_{\rm min} = 60 \, {\rm \mu m}$ and $d_{\rm max} = 600 \, {\rm \mu m}$, the evaporation times, and 'half-

life times' $T_{\rm ev1}=20$ h, $T_{\rm ev3}=30$ h, and $T_{\rm ev5}=10$ h for the fractions C⁵, C¹, and C³, respectively. For the 'long-living' fraction, C², C ⁴, C⁶ C ⁷, and C⁸, as mentioned above $T_{\rm ev4}=250$ h. A percentage ratio between C-fractions, which a priori was set initially during a distribution of droplets between fractions for the light crude oil, was the following: C¹, C², and C⁸=15%; C³ and C⁴=20%; C⁵=5%; C⁶=3%; and C⁷=7%. These ratios mean that about 40% of oil is predicted to evaporate within the few first days.

Since the transport model was designed in a z-level coordinate system, the simulated velocity and diffusivity data from POM were converted from sigma levels to z-levels, and linear interpolation between the two types of levels was implemented. The transport model had 400 vertical levels; the vertical resolution, Δz , was 0.1 m. The transport and flow models share the same horizontal resolution. Time steps for flow model were 6 and 180 s corresponding to the external and internal modes of POM, respectively, and 1800 and 180 s in simulations of droplet transport.

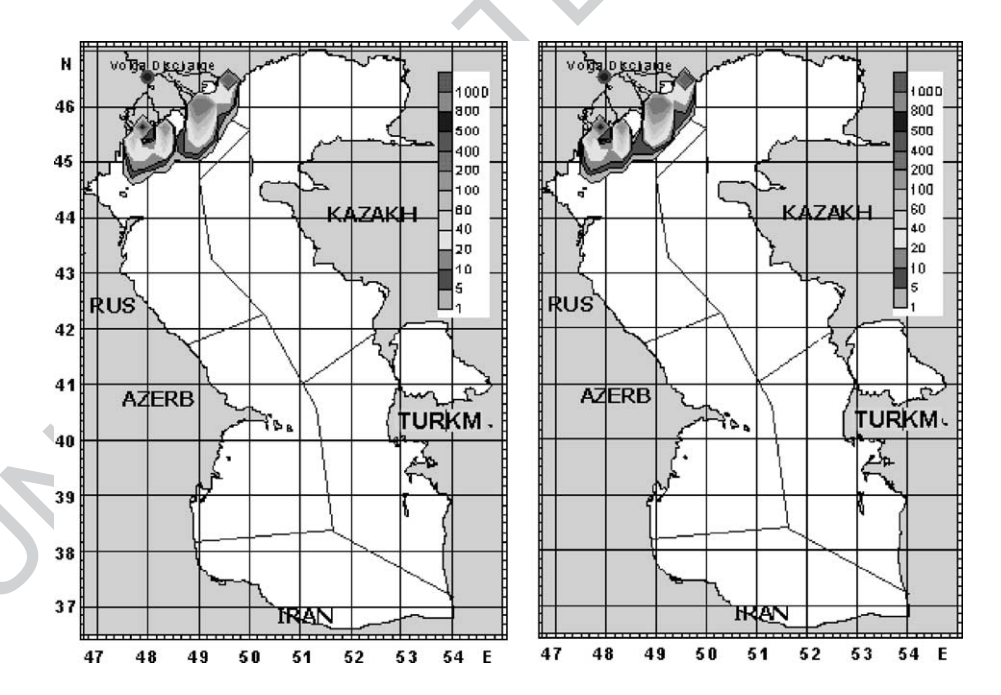


Fig. 7. Time series of the concentration of oil discharged by the Volga River for southward wind, 6.0 m/s: in 5 days (left), in 10 days (right) after release.

K.A. Korotenko et al. / Journal of Marine Systems xx (2004) xxx-xxx

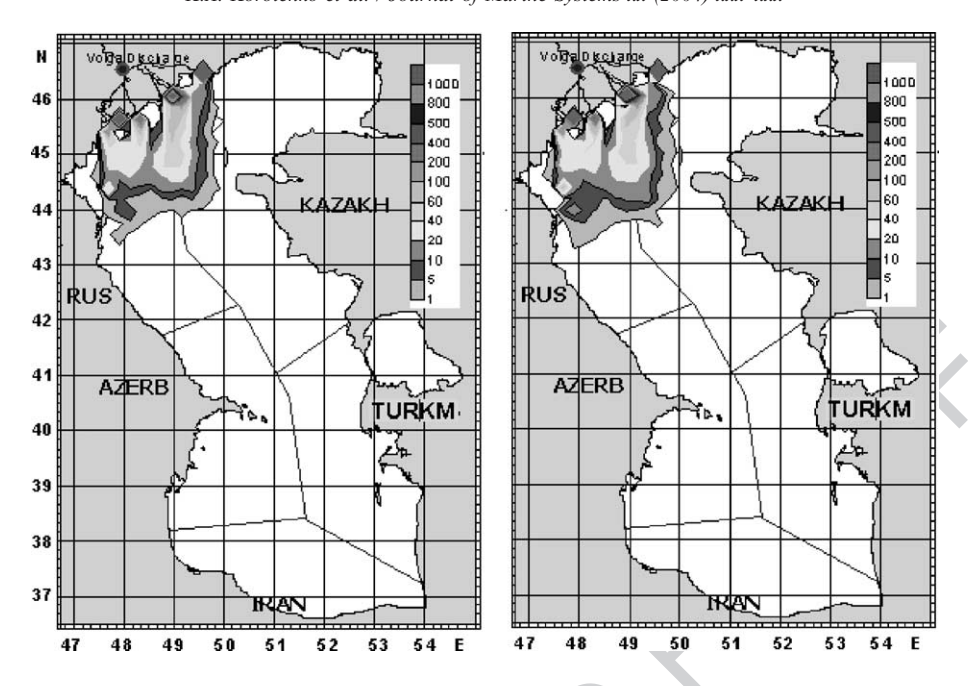


Fig. 8. The same as Fig. 7 but in 20 days (left), in 30 days (right) after release.

As was mentioned above, the total amount of oil discharged by Caspian rivers is equal approximately 75,000 tons/year (see Table 1). Among the all rivers the contribution of hydrocarbons from the Volga is equal approximately to 95% of the total petroleum input. This gives the value of 8.13 tons/h, which was

372

373

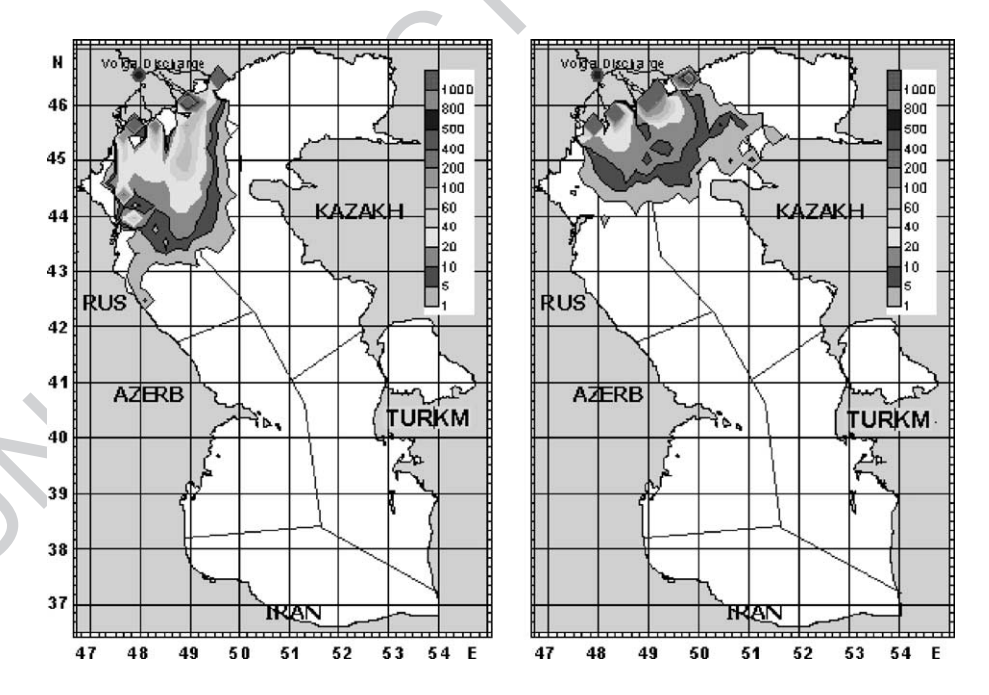


Fig. 9. Surface concentration of oil dispersed under different winds: southeastward (left) and eastward (right) winds of 6 m/s.

398

399

400

401

402

403

404

405

406

K.A. Korotenko et al. / Journal of Marine Systems xx (2004) xxx-xxx

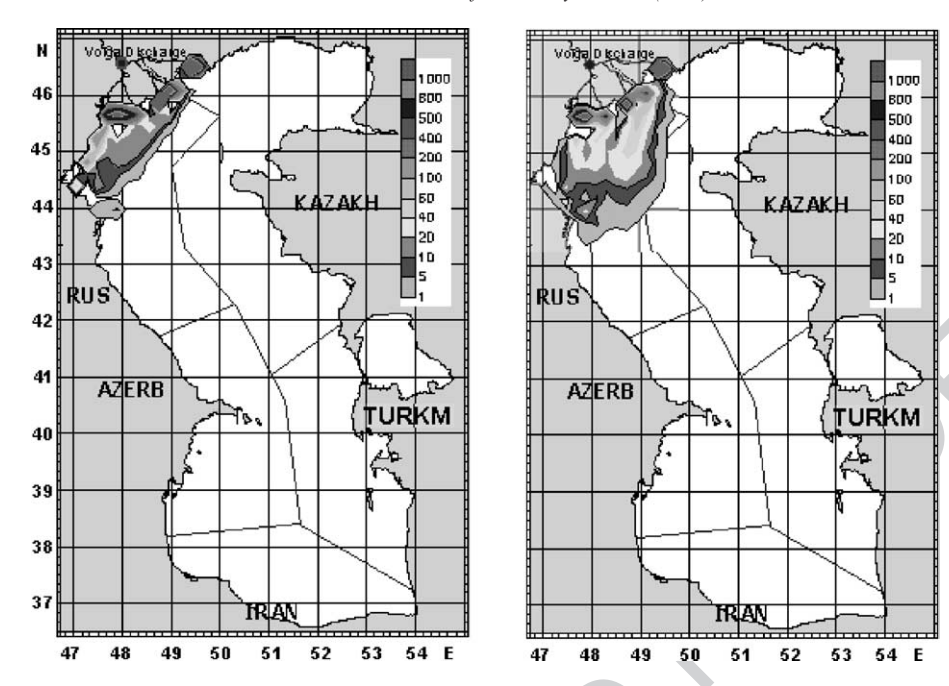


Fig. 10. Surface concentration of oil dispersed under different winds: southwestward (left) and southward (right) winds of 6 m/s.

used in numerical experiments, doing so this amount was distributed between the five passages in order to specify five-mouth river runoff. In each experiment, the calculations cover a 30-day period and carried out under different winds with the aim of assessing the probability of the cross-boundary transport, i.e., transport of oil pollution across borders of FSU¹ countries. Results are presented in Figs. 7-10. Figs. 7 and 8 depict the successive phases of the oil spill moving under climatic mean current and southward wind 6 m/ s in the 30-day release scenario. Under this wind condition, oil mostly remains in the Russian zone and some part, about 25%, of the oil pollution penetrates into the Kazakhstan zone. As is seen in Fig. 9, southeastward and particularly eastward directions of wind are predicted to be the most unfavourable for the internal waters and coast of Kazakhstan. In the case of eastward winds, the minimal time taken for the oil slick to beach oil is predicted to be about 15 days. Southward and particularly southwestward directions of wind are the most unfavourable for the Russian coast.

376

377

378

379

380

381

382

383

384

385

386

387

388

389

390

391

393

394

395

396

Fig. 11 summarizes the computed oil fate as a time history of oil emitted, oil evaporated, oil dispersed below the surface, oil beached, and oil deposited at the bottom for the experiments with the southeastward wind of 6 m/s. Fig. 11 shows an intensive depositing and beaching of oil accompanied the slick moving along the shallow zone with a depth of about 5 m. As is also seen, evaporation leads to significant mass loss for the chosen type of crude oil, i.e., more than 40%.

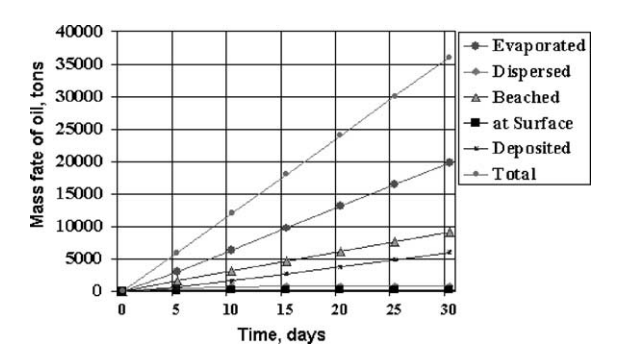


Fig. 11. Time series of oil mass components for the experiment under southwestward wind of 10 m/s.

¹ FSU is Former Soviet Union.

4. Summary 407

408 As with most of oil spill transport models, the model presented in this paper is divided into three 409 410 major modules: input, trajectory and fate prediction algorithms, and output; the latter, in turn, is subdi-411 vided into the oil data output and environmental data 412 output. The oil spill prediction procedure is split into two parts: (1) the computation of the current field by means of the Princeton Ocean Model (POM) and input of the mean currents together with winds to 416 the oil spill transport model; and (2) the oil spill model 417 which uses a random walk particle-tracking method, 418 together with the mean current from Eq. (1), to predict 419 the three-dimensional movements and fate of oil droplets. Among the processes affecting the fate of 421422 oil, advection, turbulent diffusion, evaporation, and decay are included; the decay is modelled as the 423 combined effect of all the biochemical and physical 424mechanisms that decompose oil. The combination of incident-specific environmental data and spilled oil characteristics allows conducting diagnostic and prog-427 nostic simulations of behaviour of the oil slick in the 428 marine environment. 429

The transport model has been implemented for the 431 Caspian Sea to predict oil slick movement and the area covered by the oil; also, risks coastline contamination by the beaching of offshore oil spills were 433 illustrated. Numerical experiments with 30-day scenarios of the possible oil input resulting from Volga river discharge show the potential threat caused by beaching and cross-boundary transport of the oil pollution in the northern part of the Caspian Sea.

References 439

430

434

435

436

438

- Aravamudan, K., Ray, P., Ostund, J., Newman, E., Tucker, W., 440 441 1982. Break up of oil on rough seas-simplified models and 442 step-by-step calculation. Report No CG-D28-82, U.S. Coast 443 Guard, NTIS, No. ADA118, 372.
- 444 Badalov, A.B., Rzheplinsky, D.G., 1989. Modeling of the Caspian 445 Sea upper layer dynamics under the forcing by synoptic atmo-446 spheric processes. In: Sarkisyan, A.S. (Ed.), Modeling of 447 Hydrophysical Processes and Fields in Closed Basins and Seas. 448 Nauka, Moscow, pp. 31-51 (in Russian).
- 449 Belen, M.S., Lehr, W.J., Cekirge, H.M., 1981. Spreading, disper-450 sion, and evaporation of oil slicks in the Arabian Gulf. Proc. 451 1981 Oil Spill Conference (Prevention, Behavior, Control, 452 Clean-up). 161-164.

- Blumberg, A.F., Mellor, G.L., 1987. A description of a three-dimensional coastal ocean circulation modelHeaps, N. (Ed.), Three-Dimensional Coastal Ocean Models, vol. 4. AGU, Washington. 208 pp.
- Cekirge, H.M., Palmer, S.L., 2001. Mathematical modeling of oil spilled into marine environments. In: Brebbia, C.A. (Ed.), Oil Spill Modelling and Processes. WIT Press, Southampton, pp. 124-131.
- Daling, S., Brandvik, J., Mackay, D., Johansen, Ø., 1990. Characterization of crude oils for environmental purposes. Oil and Chemical Pollution 7, 199-224.
- Hunter, J.R., 1987. Application of Lagrangian particle-tracking technique to modelling of dispersion in the sea. In: Noye, J. (Ed.), Numerical Modelling: Applications for Marine Systems. North Holland, pp. 257-269.
- Korotenko, K.A., 1994. The random walk concept in modelling matter transport and dispersion in the Sea. J. Mosc. Phys. Soc., vol. 4 (4). Allerton Press, New York, pp. 335-338.
- Korotenko, K.A., Mamedov, R.M., 2001. Modeling of oil slick transport processes in coastal zone of the Caspian Sea. Oceanology 41 (1), 37–48.
- Korotenko, K.A., Mamedov, R.M., Mooers, C.N.K., 2001. Prediction of the dispersal of oil transport in the Caspian Sea resulting from a continuous release. Spill Science and Technology Bulletin 6 (5/6), 323-339.
- Korotenko, K.A., Mamedov, R.M., Mooers, C.N.K., 2002. Prediction of the transport and dispersal of oil transport in the south Caspian Sea resulting from Blowouts. Journal of Environmental Fluid Mechanics 1 (4), 383-414.
- Korotenko, K.A., Bowman, M.J., Dietrich, D.E., 2003. Modeling of the circulation and transport of oil spills in the Black Sea. Oceanology 43 (4), 367-378.
- Kourafalou, V.H., Oey, L-Y., Wang, D.W., Lee, T.N., 1996. The fate of river discharge on the continental shelf: 1. Modeling the river plume and inner shelf coastal current. Journal of Physical Research 101 (C2), 3415-3434.
- Lehr, W.J., Belen, M.S., Cekirge, H.M., 1981. Simulated oil spills at two offshore fields in the Arabian Gulf. Marine Pollution Bulletin 12 (11), 371–374.
- Mackay, D., McAuliffe, C., 1988. Fate of hydrocarbons discharged at sea. Oil and Chemical Pollution 5, 1-20.
- Mellor, G.L., Yamada, T., 1982. Development of a turbulence closure model for geophysical fluid problems. Reviews of Geophysics and Space Physics 20, 851-875.
- Monin, A.S., Yaglom, A.M., 1965. Statistical Hydromechanics: Part I Nauka, Moscow, 640 pp.
- Proctor, R., Flather, R.A., Elliot, A.J., 1994. Modeling tides and surface drift in the Arabian Gulf—application to the Gulf Spill. Continental Shelf Research 14 (5), 531-545.
- Spaulding, M.L., 1988. A state-of-art review of oil spill trajectory and fate modeling. Oil and Chemical Pollution 4, 39-55.
- Varlamov, S.M., Yoon, J.-H., Hirose, N., Kawamura, H., 1998. . In: Garsia-Martinez, R., Brebbia, C.A. (Eds.), Oil and Hydrocarbon Spills. Modelling Analysis and Computing. Computation Mechanics Publications, Southampton, pp. 359-369.
- Yang, W.C., Wang, H., 1977. Modeling of oil evaporation in aqueous environment. Water Research 11, 879-887.

465 466 467

468 469 470

475 476 477

478 479 480

497 498 499

500 501 502